Spectroscopy and Kinetics of Wild-Type and Mutant Tyrosine Hydroxylase: Mechanistic Insight into O_2 Activation

Marina S. Chow[†], Bekir E. Eser[§], Samuel A. Wilson[†], Britt Hedman[*,‡], Keith O. Hodgson[*,†,‡], Paul F. Fitzpatrick[*,§] and Edward I. Solomon[*,†]

Supporting Information

Table S1. EXAFS Fits.

Tyrosine Hydroxylase, TH-[ ] – Resting

	fit 1 (E0 = -4.0)			fit 2 (E0 = -3.8)			**fit 3 (E0 = -.3.8)**			fit SI1 (E0 = -4.1)			fit SI2 (E0 = -3.7)		
	CN	R(Å)	($Å^2$)	CN	R(Å)	($Å^2$)	**CN**	**R(Å)**	**($Å^2$)**	CN	R(Å)	($Å^2$)	CN	R(Å)	($Å^2$)
Fe-O/N	---	---	---	---	---	---	**1**	**2.10**	**375**	2	2.12	477	1	2.08	148
Fe-O/N	6	2.15	678	5	2.15	556	**5**	**2.17**	**725**	4	2.18	830	4	2.18	420
C SS	4	3.12	774	4	3.12	776	**4**	**3.12**	**725**	4	3.12	761	4	3.12	708
C SS	4	4.08	817	4	4.08	737	**4**	**4.08**	**797**	4	4.08	819	4	4.07	733
C-N MS	8	4.39	951	8	4.40	979	**8**	**4.40**	**961**	8	4.39	945	8	4.41	987
Error			0.147			0.156			**0.145**			0.152			0.148

Tyrosine Hydroxylase, TH-[6MPH$_4$] – Cofactor

	fit 7 (E0 = -4.5)			fit 8 (E0 = -4.3)			**fit 9 (E0 = -3.7)**			fit SI3 (E0 = -3.6)			fit SI4 (E0 = -3.6)		
	CN	R(Å)	($Å^2$)	CN	R(Å)	($Å^2$)	**CN**	**R(Å)**	**($Å^2$)**	CN	R(Å)	($Å^2$)	CN	R(Å)	($Å^2$)
Fe-O/N	---	---	---	---	---	---	**1**	**2.11**	**172**	2	2.12	325	1	2.10	81
Fe-O/N	6	2.17	758	5	2.17	630	**5**	**2.20**	**785**	4	2.23	734	4	2.21	537
C SS	4	3.07	809	4	3.08	791	**4**	**3.08**	**816**	4	4.08	816	4	3.08	807
C SS	4	4.09	787	4	4.08	719	**4**	**4.08**	**654**	4	4.08	651	4	4.08	623
C-N MS	8	4.35	1045	8	4.36	1132	**8**	**4.36**	**1210**	8	4.36	1181	8	4.37	1264
Error			0.286			0.338			**0.253**			0.264			0.304

Tyrosine Hydroxylase, TH-[L-tyr, 6MPH$_4$] – Active Monodentate Glu Model

	fit 10 (E0 = -4.1)			fit 11 (E0 = -3.8)			fit SI5 (E0 = -3.9)			**fit 12 (E0 = -4.3)**			fit SI6 (E0 = -4.7)		
	CN	R(Å)	($Å^2$)	CN	R(Å)	($Å^2$)	CN	R(Å)	($Å^2$)	**CN**	**R(Å)**	**($Å^2$)**	CN	R(Å)	($Å^2$)
Fe-O/N	---	---	---	---	---	---	1	1.57	4606	**1**	**2.00**	**411**	1	2.00	428
Fe-O/N	6	2.13	1127	5	2.13	932	5	2.13	933	**4**	**2.15**	**567**	4	2.15	559
C SS	4	3.11	663	4	3.11	602	4	3.11	585	**4**	**3.10**	**664**	2	3.10	121
C SS	4	4.07	886	4	4.06	818	4	4.05	710	**4**	**4.06**	**867**	2	4.02	91
C-N MS	8	4.37	778	8	4.38	771	8	4.38	766	**8**	**4.37**	**769**	4	4.39	132
Error			0.272			0.203			0.169			**0.190**			0.163

Tyrosine Hydroxylase, TH-[L-tyr, 6MPH$_4$] – Active Bidentate Glu Model

	fit 13 (E0 = -4.9)			fit 14 (E0 = -4.6)			fit SI7 (E0 = -4.3)			**fit 15 (E0 = -4.3)**			fit SI8 (E0 = -3.9)		
	CN	R(Å)	($Å^2$)	CN	R(Å)	($Å^2$)	CN	R(Å)	($Å^2$)	**CN**	**R(Å)**	**($Å^2$)**	CN	R(Å)	($Å^2$)
Fe-O/N	---	---	---	1	2.04	408	1	2.03	263	**2**	**2.05**	**578**	2	2.06	673
Fe-O/N	5	2.14	943	4	2.17	782	4	2.18	269	**3**	**2.15**	**628**	3	2.15	882
C SS	1	2.54	336	1	2.50	342	1	2.47	99	**1**	**2.53**	**372**	1	2.49	111
C-O MS	4	2.63	336	4	2.68	342	4	2.73	99	**4**	**2.65**	**372**	4	2.74	111
C SS	4	3.10	708	4	3.10	821	2	3.11	337	**4**	**3.11**	**733**	2	3.11	298
C SS	4	4.05	794	4	4.05	745	2	4.03	28	**4**	**4.05**	**760**	2	4.04	58
C-N MS	8	4.38	810	8	4.38	823	4	4.40	165	**8**	**4.39**	**769**	4	4.40	189
Error			0.124			0.119			0.093			**0.090**			0.075

Some fits from text are reprinted here for convenience of comparison. Fits are numbered in two ways: Those that appear in text are listed with the corresponding number, and those only shown in Supporting Information are labeled with the pre-fix "SI". Fits that are listed as the "best fit" in text are shown in bold. TH-[ ] is known to be 6C according to MCD and XAS Pre-edge. The Debye-Waller factors and fit can be used as a reference to compare other fits of other TH complexes. TH-[6MPH$_4$] does not fit to a 1:4, 5C, split shell, as does active, making it clearly 6C. TH-[L-tyr, 6MPH$_4$] fits where the ligand lost on the conversion from 6C to 5C is His, results in Debye-Waller factors which are unrealistic for outer sphere components when the model is fit with either a 1:4, or 2:3 split in the first shell despite any improvement in the error.

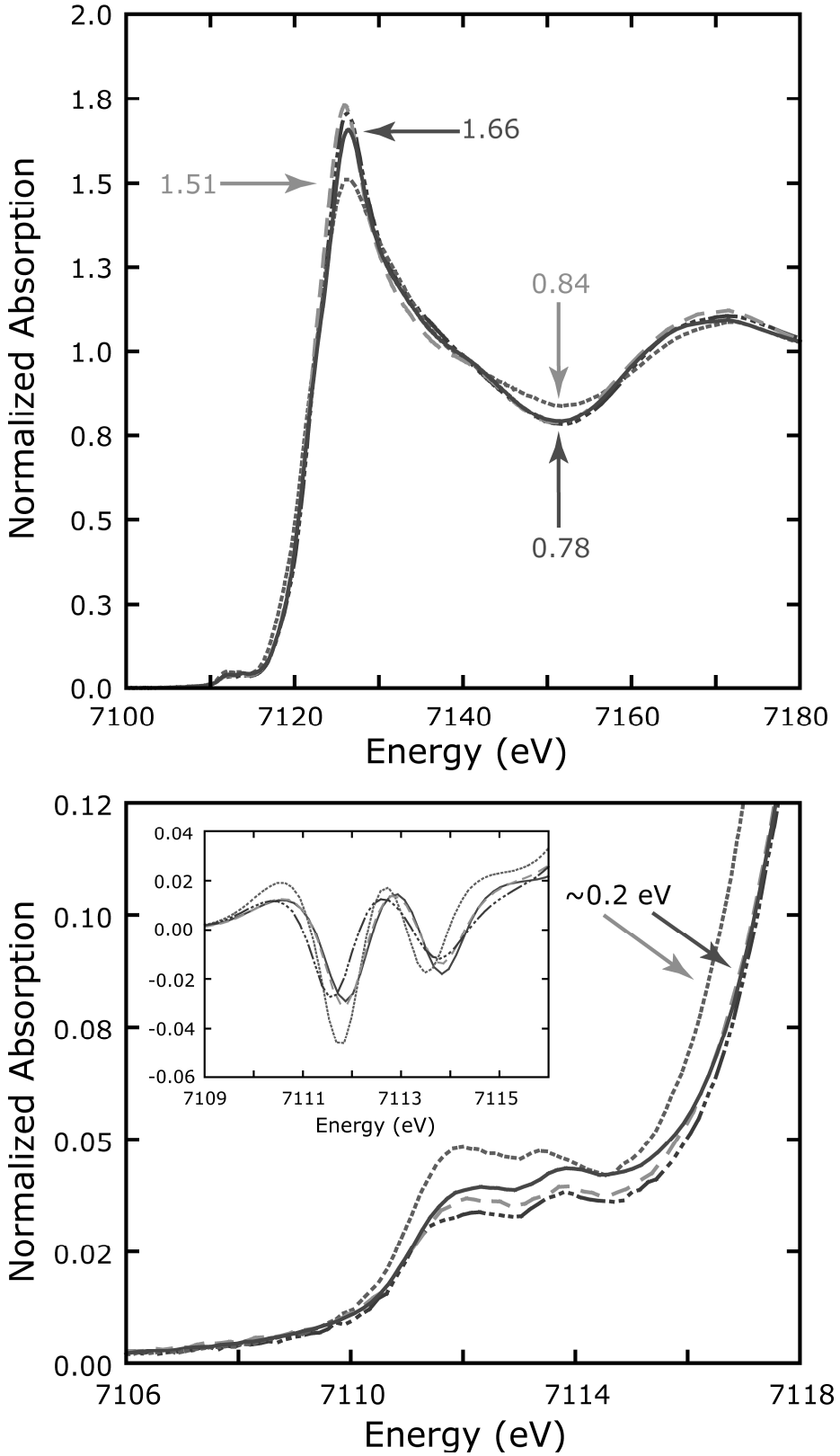

Figure S1. Fe K edge and pre-edge spectra of TH-[ ] (—), TH-[L-tyr] (···—···), TH-[6MPH$_4$] (- - -) and TH-[L-tyr, 6MPH$_4$] (----). This is a black and white rendition of Figure 1 in the text.

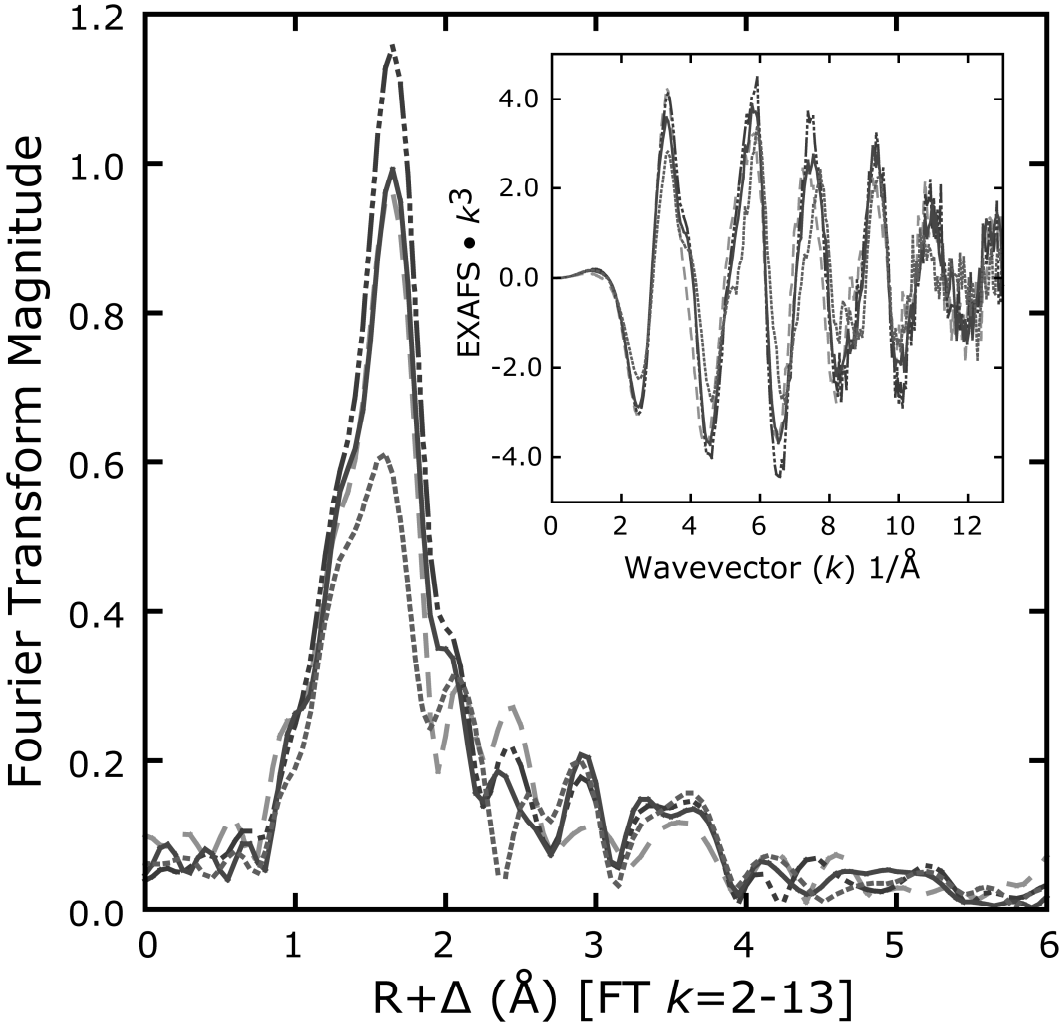

Figure S2. Fourier transforms to k = 13 Å^{-1} for tyrosine hydroxylase. TH-[ ] (—), TH-[L-tyr] (···—···), TH-[6MPH$_4$] (- - -) and TH-[L-tyr, 6MPH$_4$] (----). This is a black and white rendition of Figure 2 in the text.

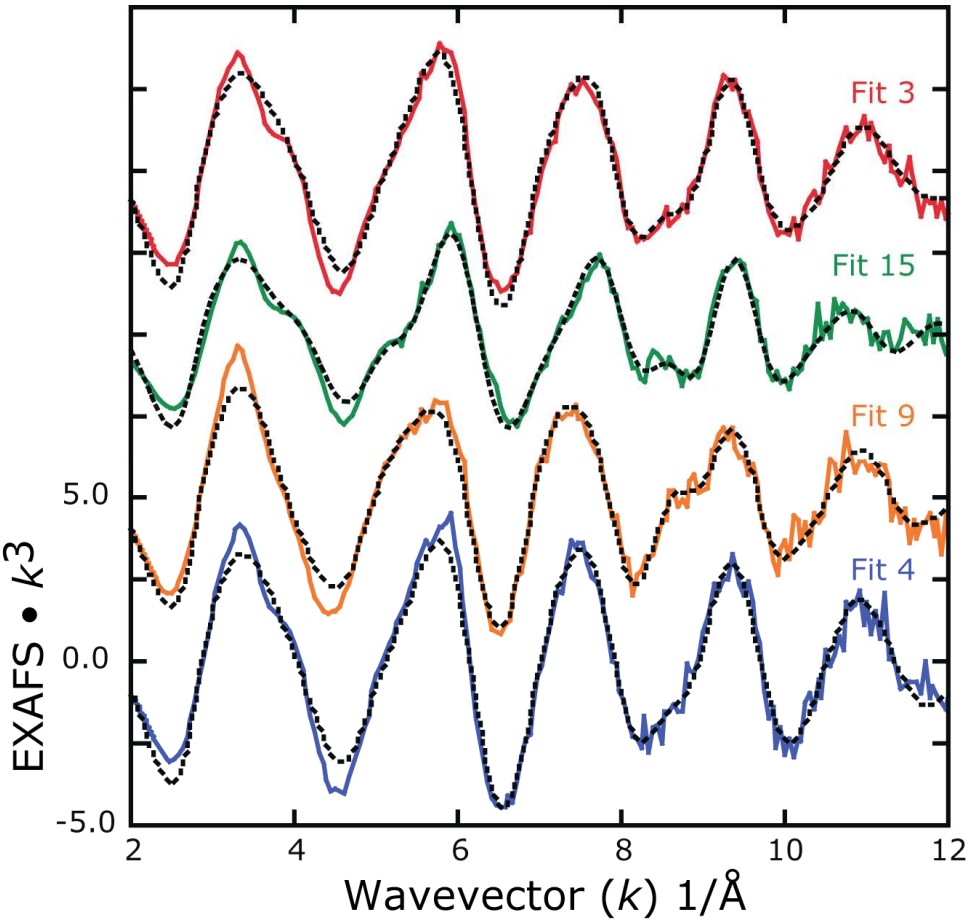

Figure S3. *K*-space data and best fits from the text for TH-[ ] (red), TH-[L-tyr, $6MPH_4$] (green), TH-[$6MPH_4$] (orange), and TH-[L-tyr] (blue). Fit numbers are listed corresponding to data and fit.

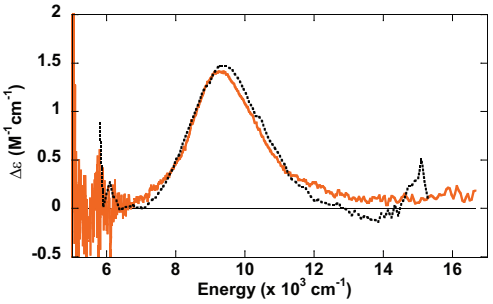

Figure S4. MCD spectrum of TH-[5-deaza-6MPH$_4$] (black dotted line) compared to TH-[6MPH$_4$] (orange solid line).

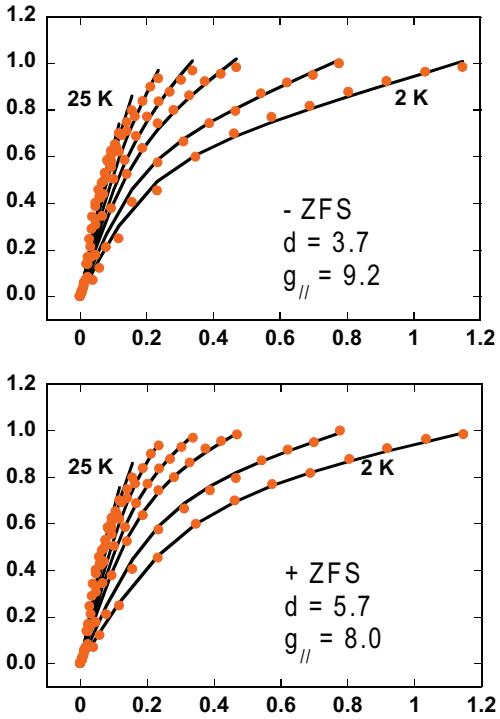

Figure S5. TH-[6MPH$_4$] VTVH MCD data and +/- ZFS fits at 8230 cm^{-1}.

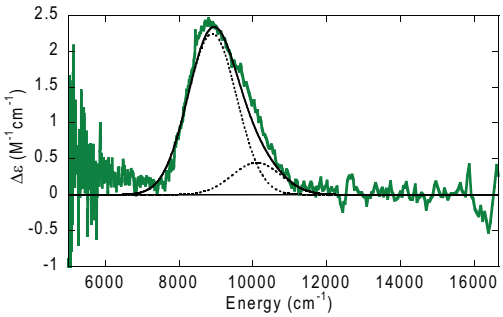

Figure S6. The MCD spectrum of Fe^{II}TH[tyr,6MPH$_4$] (green) is fit with two Gaussian bands (dotted lines) to yield the generated best fit spectrum (solid black line).

Table S1. Ligand field parameters for TH mutants

Sample	Band 1 (cm^{-1})	Band 2 (cm^{-1})	10 Dq (cm^{-1})	Δ^5E_g (cm^{-1})
E332A TH-[ ]	8720	10750	9735	2030
E332A TH-[L-tyr, $6MPH_4$]	9390	10950	10170	1560
S395A TH-[ ]	9250	10860	10055	1610
S395A TH-[L-tyr, $6MPH_4$]	8960	–	–	> 4000

Table S2. Spin Hamiltonian and ground state parameters for TH mutants.

Sample	d	g//	D	|E|	Δ	V	V/2Δ
E332A TH-[ ]	3.8	9.1	–	–	-200	80	0.20
E332A TH-[L-tyr, $6MPH_4$]	5.5	8	12.8	3.2	600	400	0.33
S395A TH-[ ]	3.2	9.3	–	–	-300	90	0.15
S395A TH[L-tyr, $6MPH_4$]	7.4	8	12.9	2.2	500	240	0.24

Values in cm^{-1}

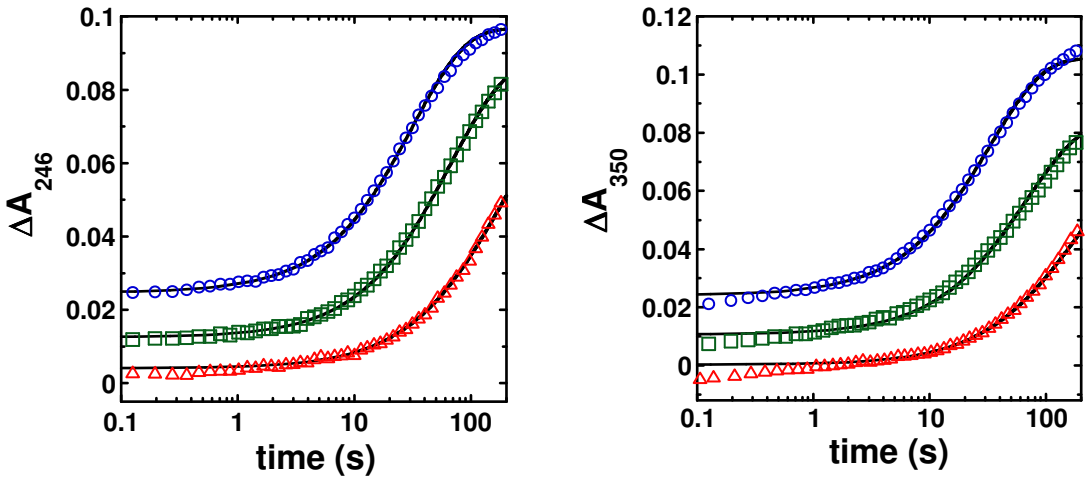

Figure S7: Stopped-flow absorbance traces at 246 (left) and 350 nm (right), acquired by mixing an anaerobic solution of ~ 120 μM (final) Fe^{II}TH-[ ] in 200 mM Hepes, 10% glycerol and 0.1 M KCl, pH 7.5, with an equal volume of oxygenated buffer at 5 ºC. The symbols are the experimental data at final O_2 concentrations of 950 (blue circles), 480 (green squares), or 120 μM (red triangles). The solid lines are simulations according to the mechanism of Scheme 3A, using extinction coefficients from Figure 11.

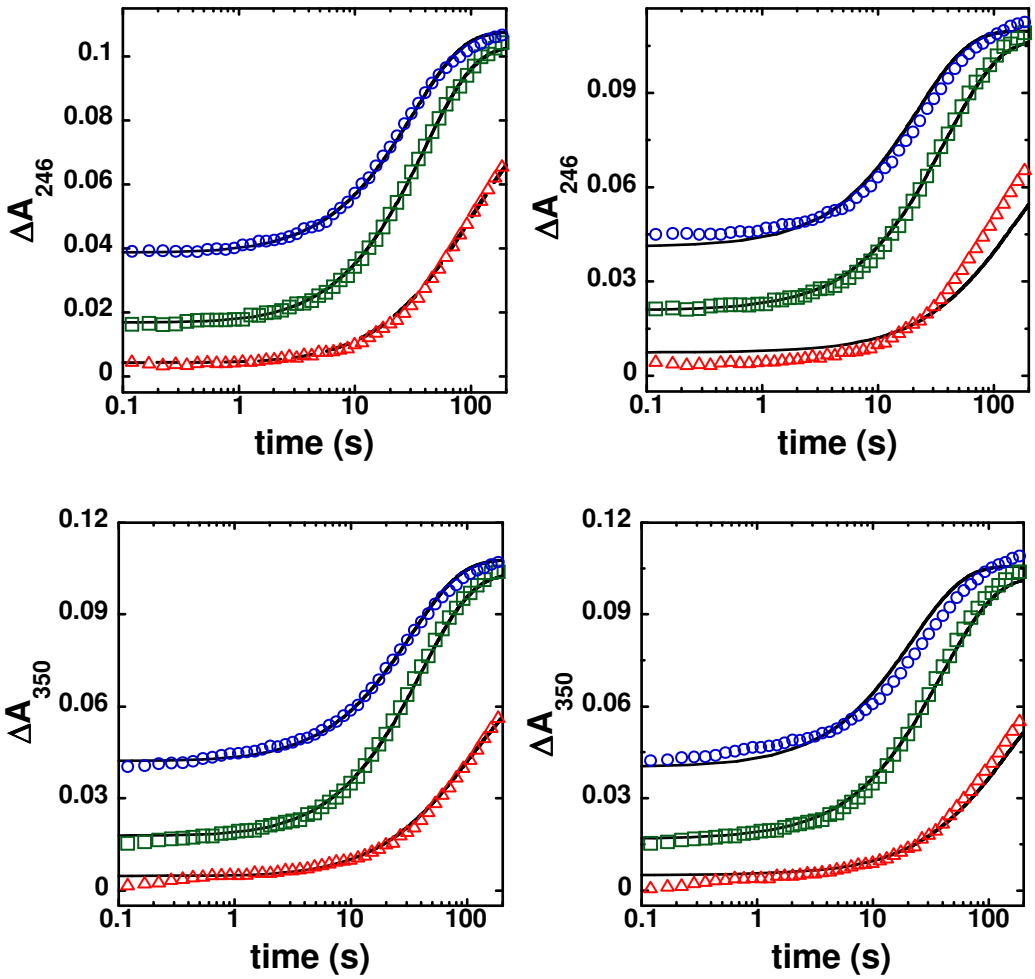

Figure S8: Stopped-flow absorbance changes at 246 and 350 nm upon mixing an anaerobic solution of ~ 85 μM (final) WT Fe^{II}TH-[L-tyr] in 200 mM Hepes, 10% glycerol and 0.1 M KCl, pH 7.5, with an equal volume of oxygenated buffer at 5 ºC. The symbols are the experimental data with final O_2 concentrations of 950 (blue circles), 480 (green squares), or 95 μM (red triangles). The solid lines are simulations using mechanism C (left) or D.

Mechanism C:

TH:Fe(II):L-tyr + O_2 ⇔ TH:Fe(II):L-tyr:O_2 $k_1 = 2\ mM^{-1}s^{-1}$ $k_{-1} = 0.5\ s^{-1}$

TH:Fe(II):L-tyr:O_2 → TH:Fe(III):L-tyr $k_2 = 0.04\ s^{-1}$

Mechanism D:

TH:Fe(II):L-tyr + O_2 → TH:Fe(III):L-tyr $k = 0.055\ mM^{-1}s^{-1}$

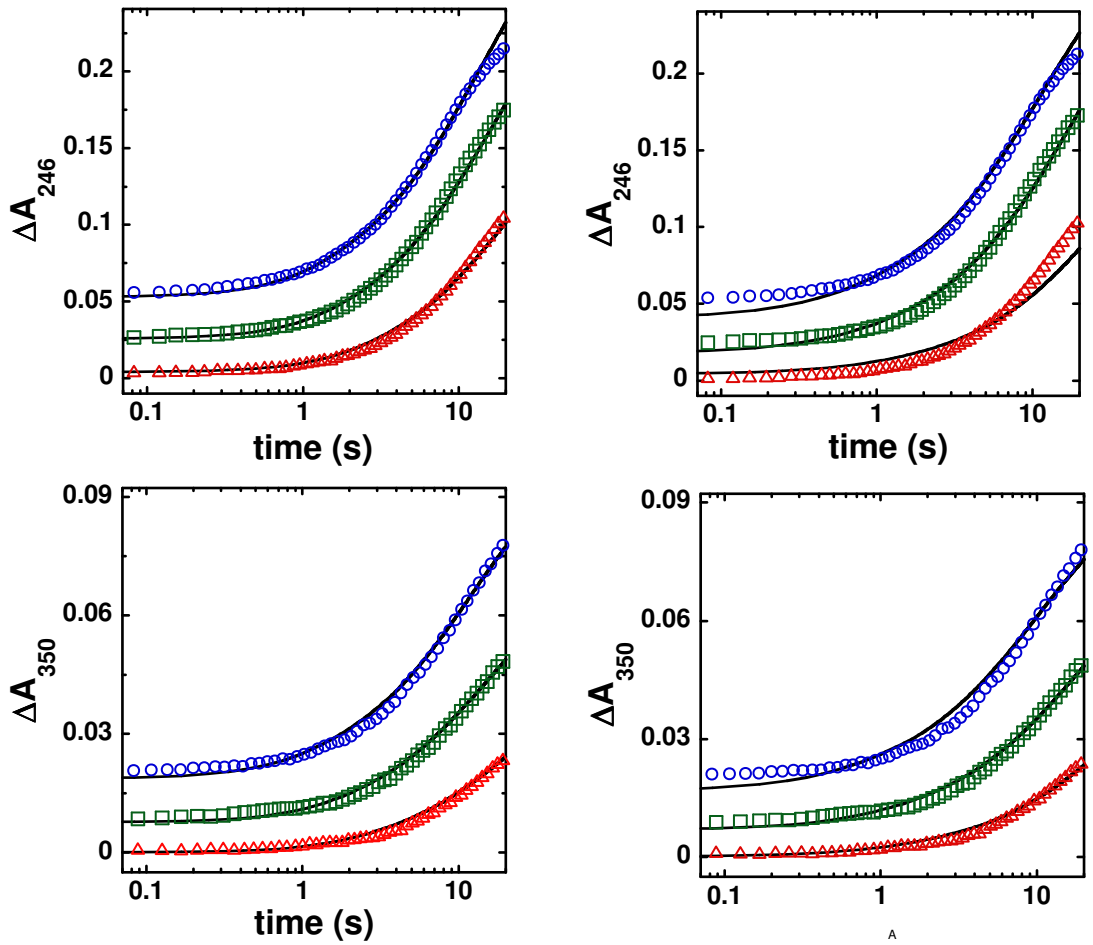

Figure S9: Stopped-flow absorbance traces at 246 and 350 nm upon mixing an anaerobic solution of ~ 150 μM (final) WT Fe^{II}TH-[$6MPH_4$] in 200 mM Hepes, 10% glycerol and 0.1 M KCl, pH 7.5, with an equal volume of oxygenated buffer at 5 ºC. The symbols are the experimental data at final O_2 concentrations of 950 (blue circles), 480 (green squares), or 190 μM (red triangles). The solid lines are simulations using mechanism A below (left panels) or B (right). The final step for both mechanisms is the oxidation of $6MPH_4$-free enzyme (TH:Fe(II)) present in the reaction mixture. The extinction coefficients used as parameters were from Figure 11. The extinction coefficient for $6MPH_3^{\bullet}$ was taken from *Patel, et. al. Free Radical Biology & Medicine* ***2002****, 32, 203-211.*

Mechanism A:

TH:Fe(II):$6MPH_4$ + O_2 ⇔ TH:Fe(II):$6MPH_4$:O_2 $k_1 = 1.5\ mM^{-1}s^{-1}$ $k_{-1} = 0.5\ s^{-1}$

TH:Fe(II):$6MPH_4$:O_2 → TH:Fe(III) + $6MPH_3^{\bullet}$ + H_2O_2 $k_2 = 0.16\ s^{-1}$

$6MPH_3^{\bullet}$ + $6MPH_3^{\bullet}$ → $6MPH_4$ + q-$6MPH_2$ $k_3 = 40\ mM^{-1}s^{-1}$

TH:Fe(II) + O_2 → TH:Fe(III) $k_4 = 0.037\ mM^{-1}s^{-1}$

Mechanism B:

TH:Fe(II):$6MPH_4$ + O_2 → TH:Fe(III) + $6MPH_3^{\bullet}$ + H_2O_2 $k_1 = 0.16\ mM^{-1}s^{-1}$

$6MPH_3^{\bullet}$ + $6MPH_3^{\bullet}$ → $6MPH_4$ + q-$6MPH_2$ $k_2 = 40\ mM^{-1}\ s^{-1}$

TH:Fe(II) + O_2 → TH:Fe(III) $k_3 = 0.037\ mM^{-1}\ s^{-1}$

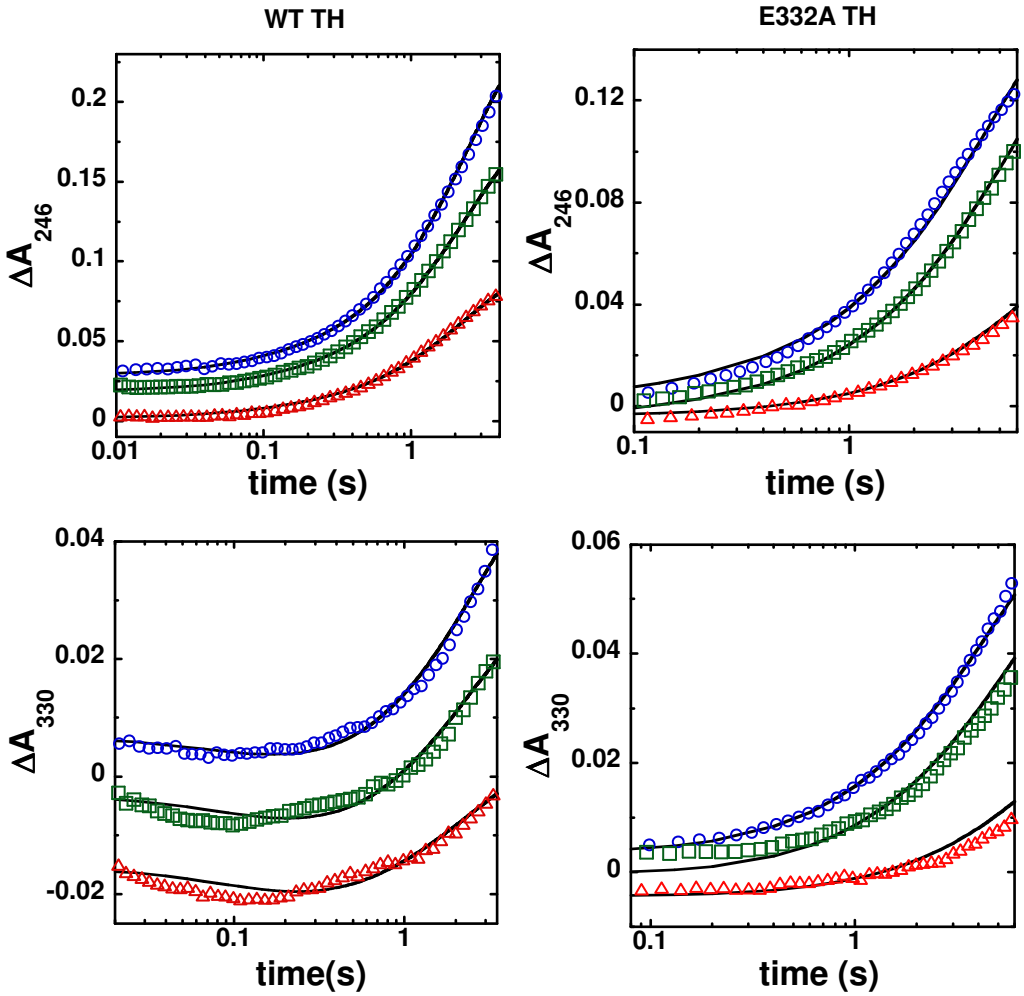

Figure S10: Stopped-flow absorbance traces at 246 and 330 nm for WT TH (left) and for E332A TH (right) upon mixing an anaerobic solution of Fe^{II}TH-[L-tyr,6MPH$_4$] (160 μM final for WT and 125 μM final for E332A) in 200 mM Hepes, 10% glycerol and 0.1 M KCl, pH 7.5, with an equal volume of oxygenated buffer at 5 ºC. The symbols are the experimental data with final O_2 concentrations of 140 (blue circles), 95 (green squares) and 50 μM (red triangles) for WT TH and 950 (blue circles), 480 (green squares), or 190 μM (red triangles) for E332A TH. The solid lines are simulations using the mechanisms below. The extinction coefficients were from Figure 11. For unknown extinction coefficients, global analysis was used to obtain initial estimates. The first step in the WT TH mechanism is the reversible formation of an oxygen complex prior to the first observable absorbance change, the O-O bond cleavage step that results in Fe^{IV}=O and 4a-HO-pterin. The rate constant of 24 s^{-1} for this step was directly taken from an earlier study in which the Fe^{IV}=O formation and decay and DOPA formation were fit simultaneously[26]. No absorbance change associated with the formation of the Fe-OO-pterin could be detected, so we assume that this step occurs after the reversible formation of the initial oxygen adduct, with a rate constant faster than 24 s^{-1}. A third step with a rate constant of 0.42 s^{-1} was necessary to account for the absorbance change at later time points, and was attributed to product release step.

The decay of Fe^{IV}=O to form the product DOPA was not included in this model, since there is no detectable absorbance change for these species. The slow formation of the q-$6MPH_2$ (~$0.02s^{-1}$) at later time points was omitted in this analysis. The E332A TH reaction was modeled similarly to WT TH, except that the final two steps were replaced by a single step corresponding to the formation of a hydroperoxy-pterin (HOO-$6MPH_3$).

WT TH

TH:Fe(II):$6MPH_4$:L-tyr + O_2 ⇔ TH:Fe(II):$6MPH_4$:L-tyr :O_2	$k_1 = 300\ mM^{-1}s^{-1}$ $k_{-1} = 50\ s^{-1}$
TH:Fe(II):$6MPH_4$:L-tyr :O_2 → TH:Fe(IV)=O + 4a-OH-$6MPH_3$	$k_2 = 24\ s^{-1}$
4a-OH-$6MPH_3$ → 4a-OH-$6MPH_3$ *	$k_3 = 0.42\ s^{-1}$

E332A TH

TH:Fe(II):$6MPH_4$:L-tyr + O_2 ⇔ TH:Fe(II):$6MPH_4$:L-tyr :O_2	$k_1 = 10\ mM^{-1}s^{-1}$ $k_{-1} = 3\ s^{-1}$
TH:Fe(II):$6MPH_4$:L-tyr :O_2 → TH:Fe(II) + HOO-$6MPH_3$	$k_2 = 0.3\ s^{-1}$

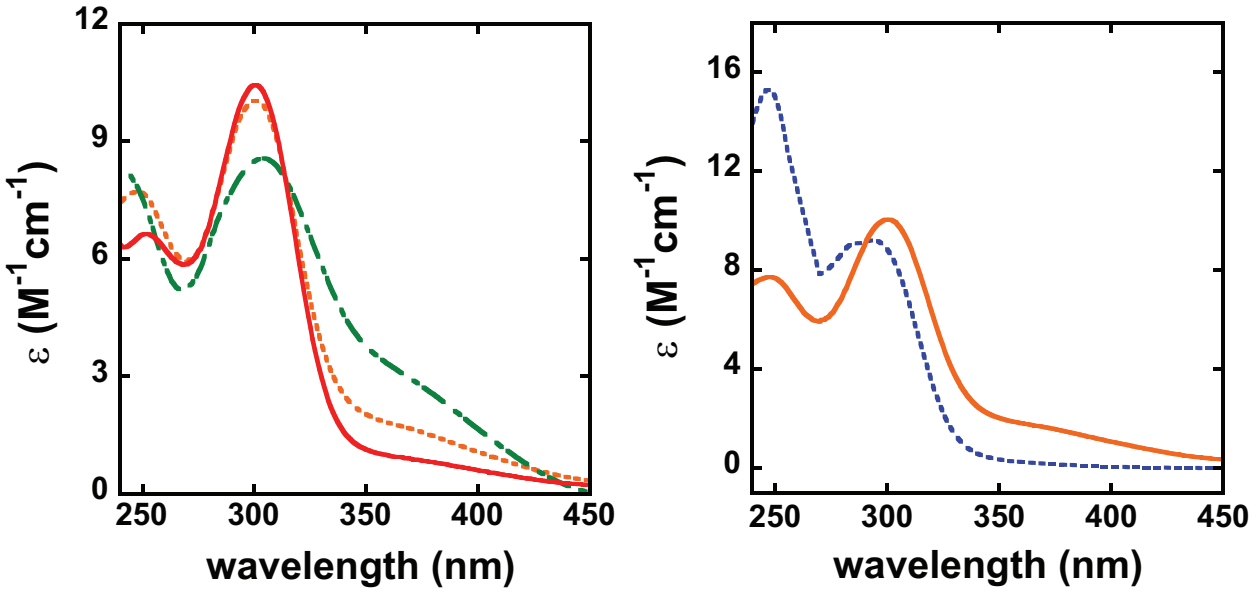

Figure S11: UV-Visible spectra of intermediates in the E332A TH reaction. Left panel: Spectra of intermediates calculated by fitting the absorbance changes during E332A TH turnover to the model below. UV-Visible spectra between 240 and 450 nm during the reaction of 40 μM $6MPH_4$, 10 μM E332A TH, 200 μM tyrosine, 250 μM oxygen, in 10 μM ferrous ammonium sulfate, 200 mM Hepes at pH 8.0 and 25 ºC, were obtained at 1 s intervals using a diode array spectrophotometer for a total of 400 s. The spectra were fit globally by the program Specfit (Spectrum Software Associates) to the three step kinetic mechanism below. The spectra that are shown are for $6MPH_4$ (red, —), A (orange, ---) and B (green, ···—···). Right panel: Comparison of intermediate A (orange, —) spectrum with that of 4a-HO-$6MPH_3$ (blue, ---).

$$\mathbf{6MPH_4} \xrightarrow{k_1} \mathbf{A} \xrightarrow{k_2} \mathbf{B} \xrightarrow{k_3} \mathbf{C}$$